# Azophosphines

Jordan, Emma; Calder, Ethan; Adcock, Holly; Male, Louise; Nieger, Martin; Slootweg, Chris; Jupp, Andrew

*DOI:*
10.26434/chemrxiv-2024-4kmw8



*Document Version*
Other version

*Citation for published version (Harvard):*
Jordan, E, Calder, E, Adcock, H, Male, L, Nieger, M, Slootweg, C & Jupp, A 2024 'Azophosphines: Synthesis, Structure and Coordination Chemistry' ChemRxiv. https://doi.org/10.26434/chemrxiv-2024-4kmw8

# Azophosphines: Synthesis, Structure and Coordination Chemistry

Emma J. Jordan,[a] Ethan D. E. Calder,[a] Holly V. Adcock,[a] Louise Male,[a] Martin Nieger,[b] J. Chris Slootweg,[c] Andrew R. Jupp*[a]

[a] School of Chemistry, University of Birmingham, Edgbaston, Birmingham, B15 2TT, UK

[b] Department of Chemistry, University of Helsinki, A. I. Virtasen aukio 1, 00014 Helsinki, Finland

[c] Van 't Hoff Institute for Molecular Sciences, University of Amsterdam, PO Box 94157, 1090 GD Amsterdam, The Netherlands

**Abstract**: The conceptual replacement of nitrogen with phosphorus in common organic functional groups unlocks new properties and reactivity. The phosphorus-containing analogues of triazenes are underexplored but offer great potential as flexible and small bite-angle ligands. This manuscript explores the synthesis and characterisation of a family of air-stable azophosphine-borane complexes, and their subsequent deprotection to the free azophosphines. These compounds are structurally characterised, both experimentally and computationally, and highlight the availability of the phosphorus lone pair for coordination. This is confirmed by demonstrating that neutral azophosphines can act as ligands in Ru complexes, and can coordinate as monodentate or bidentate ligands in a controlled manner, in contrast to their nitrogen analogues.

## Introduction

Functional groups are the cornerstone of predicting and rationalising reactivity in synthetic chemistry. The conceptual replacement of 2p elements in common functional groups with heavier main-group congeners can lead to drastically different properties and reactivity. The study of phosphorus-containing analogues of nitrogen-containing moieties has grown in recent years, with examples including phosphorus analogues of pyridine and urea (Figure 1), as well as imines, nitriles, and the cyanate and cyanide anions.[1] When phosphorus is in a low-coordinate environment, it has been shown that it is more similar to carbon than to nitrogen, principally due to the isolobal nature of P and C and their similar electronegativities, resulting in phosphorus being dubbed the *carbon copy*.[2] For tri-coordinate phosphorus, the presence of the lone pair means that there are obvious parallels with analogous nitrogen compounds, although there is a significantly reduced propensity for delocalisation of this lone pair in the former. For example, in *N*,*N*-dimethylformamide (DMF), the nitrogen is planar and the methyl groups are inequivalent due to significant C–N double bond character, whereas in the heavier *P*,*P*-dimethylformylphosphine the phosphorus moiety is pyramidal and there is minimal donation of the lone pair into the C=O π* orbital (Figure 1C).[3]

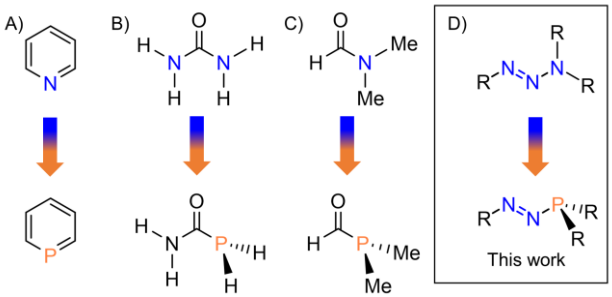


**Figure 1**. Phosphorus-containing analogues of pyridine (A), urea (B), DMF (C) and triazene (D).

Triazenes (RN=N–NR'$_2$; Figure 1D) are a common functional group in organic chemistry, and can be found in dyes and pharmaceuticals, such as the anti-

cancer medications *Temozolomide* and *Dacarbazine*.[4] They are also versatile tools in organic synthesis, where the triazene moiety can act as a robust protecting group for amines, or as a precursor in numerous synthetic transformations.[5] The literature on the coordination chemistry of neutral triazenes is scant. All examples feature monodentate coordination to the metal centre *via* the terminal imino nitrogen, and there are no examples of binding through the tri-coordinate amino nitrogen centre.[6] *N*,*N*'-disubstituted triazenes are much more commonly deprotonated to afford anionic triazenides ([RNNNR]$^-$), which can then act as monodenate, bidentate and bridging ligands to a wide range of metal centres.[7] Triazenides are isoelectronic with amidinates ([RNC(R')NR]$^-$), but the central electronegative nitrogen in triazenides results in a reduced charge density of the terminal nitrogen atoms relative to amidinates, which would confer an increased electrophilicity at the ligated metal centre.[8]

The conceptual replacement of the tri-coordinate nitrogen centre in triazenes with a phosphorus atom yields azophosphines: RN=N–PR'$_2$ (Figure 1D). Azophosphines were first synthesised in the late 1970s by Wiberg and co-workers by the reaction of silyldiazenes and chlorophosphines,[9] and alkenyl-substituted variants were subsequently prepared by Attanasi and co-workers.[10] It was over 30 years later that this family of molecules were revisited, when Cummins and co-workers synthesised and crystallographically characterised Mes$N_2$P**A** (Mes = mesityl, **A** = anthracene, Scheme 1A).[11] This molecule was prepared in 14% yield and was thermally unstable due to loss of the labile anthracene moiety, which enabled the molecule to act as a synthetic equivalent of mesitylphosphaazide (Mes$N_2$P) in a range of cycloaddition reactions. The Cummins group also recently published the synthesis of a wider family of azophosphines, and explored their reactivity with alkynes to afford N-heterocyclic iminophosphoranes.[12] The azophosphines were synthesised in two different ways. The first method was analogous to Wiberg's approach[9] involving the reaction of silyldiazenes and chlorophosphines, although this method was unsuccessful for sterically hindered chlorophosphines such as $^i$Pr$_2$PCl. The second approach involved oxidation of phosphinohydrazines with benzoquinones (BQ) and could tolerate the larger P-substituents $^i$Pr and Cy (cyclohexyl), although the size of the BQ had to be tailored to the steric profile of the azophosphine (Scheme 1B). A general synthetic route to this family of compounds that tolerates bulky groups is still missing.

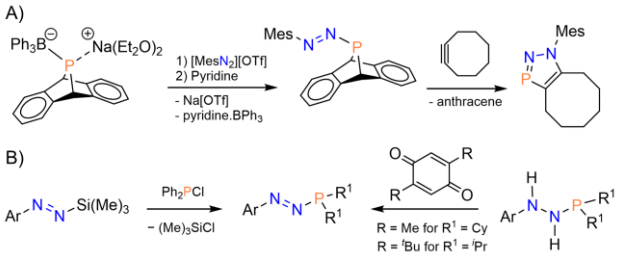


**Scheme 1.** Previous syntheses of azophosphines. Synthesis of Mes$N_2$P**A** (A); using silyldiazenes and chlorophosphines (left to right), and oxidation of a phosphinohydrazine (right to left) (B).

This manuscript explores the synthesis and characterisation of a family of air-stable azophosphine-borane complexes, and their subsequent deprotection to the free azophosphines. These compounds are structurally characterised, both experimentally and computationally, and highlight the availability of the phosphorus lone pair for coordination. This is confirmed by demonstrating that neutral azophosphines can coordinate to a ruthenium(II) centre as both a mono- and bidentate ligand.

## Results & Discussion

We sought to develop a simple synthetic procedure for azophosphines that would be tolerant to bulky groups on the phosphorus centre. Azophosphonium cations, [Ar-N=N-P$R_3$]$^+$, have recently been synthesised and are readily accessible by simple addition of a tertiary phosphine (P$R_3$) to an arenediazonium salt.[13] In our hands, the analogous reactivity of a secondary phosphine (HP$R_2$) with arenediazonium cations (for subsequent deprotonation to the neutral azophosphine) led to uncontrolled reactivity and decomposition. Similarly unsuccessful results were observed for direct reactions of phosphide anions ([P$R_2$]$^-$) with diazonium salts, which we postulate is due to single-electron transfer processes and subsequent decomposition of the neutral diazenyl radical.

It was observed that coordination of the secondary phosphine to the parent borane $BH_3$ could temper and control the reactivity. $HPPh_2{\cdot}BH_3$ was deprotonated with *sec*-BuLi at –78 °C, and this was added dropwise to a stirring suspension of mesitylenediazonium tetrafluoroborate in THF at –78 °C to give an immediate purple colour and the formation of the target azophosphine-borane complex $MesN_2PPh_2{\cdot}BH_3$ (**1·BH₃**) (Scheme 2). A broad quartet signal was observed at 75.8 ppm by $^{31}P\{^1H\}$ NMR spectroscopy, consistent with the P–B coupling expected for the product. The borane group renders **1·BH₃** air-stable enough to be purified by column chromatography and the product was isolated as a purple solid in 42% yield.

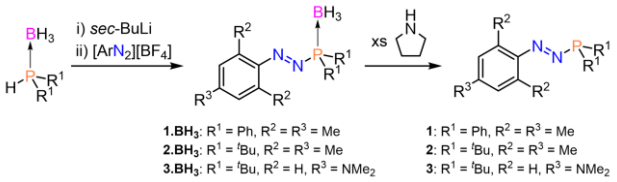


**Scheme 2.** General synthesis of azophosphine-boranes, and subsequent deprotection to the corresponding azophosphine, which is tolerant to bulky P-substituents.

To assess whether this synthetic procedure would tolerate a large degree of steric bulk on the P and N substituents, the analogous reaction of $HP^tBu_2{\cdot}BH_3$ with $[MesN_2][BF_4]$ was attempted, and gratifyingly gave $MesN_2P^tBu_2{\cdot}BH_3$ (**2·BH₃**) as a purple solid after work-up in 55% yield (Scheme 2). To etsablish that the Mes group on the nitrogen is not a prerequisite for the formation of azophosphine boranes, (*p*-$NMe_2$)$C_6H_4N_2P^tBu_2{\cdot}BH_3$ (**3·BH₃**) was prepared from the corresponding diazonium salt as a red solid in an excellent yield of 84% (Scheme 2).

The three azophosphine-borane complexes were characterised by single crystal X-ray diffraction (SXRD) (Figure 2A-C). The P1–$C_{Ar}$ bond lengths of **1·BH₃** (1.7997(11) Å, 1.8021(11) Å) are subtly shorter than the corresponding P1–$C_{tBu}$ bond lengths of **2·BH₃** (1.862(6) Å, 1.844(6) Å), suggesting that, despite donation of the P1 electron lone pair to B1, for **1·BH₃**, there is also some delocalisation into the P1-phenyl substituents. The P1–N1 bond length of **3·BH₃** (1.7380(12) Å) is statistically shorter, and the N1–N2 bond length (1.2681(17) Å) longer, than that of **2·BH₃** (1.769(5) Å, 1.226(6) Å, respectively). This is rationalised by the mesomeric effect of the electron lone pair of N3 in **3·BH₃**.

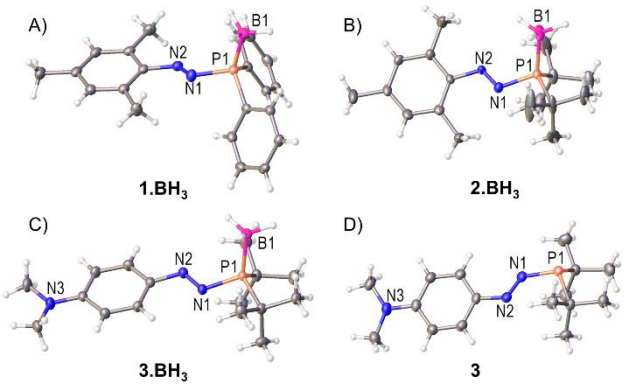


**Figure 1.** Single crystal structures of **1·BH₃** (A); **2·BH₃** (B); **3·BH₃** (C); **3** (D). Selected bond distances (Å) and angles (°): **1·BH₃** N1–N2 1.2504(14), N1–P1 1.7565(10), P1–N1–N2 115.00(8); **2·BH₃** N1–N2 1.226(6), N1–P1 1.769(5), P1–N1–N2 113.5(4); **3·BH₃** N1–N2 1.2681(17), N1–P1 1.7380(12), P1–N1–N2 114.33(10); **3** N1–N2 1.258(3), N1–P1 1.7494(18), P1–N1–N2 119.34(14). Thermal ellipsoids were drawn at the 50% probability level.[14]

The borane protecting group could be fully removed using the nucleophilic amine pyrrolidine.[15] Treatment of **1·BH₃** with an excess of pyrrolidine resulted in a small shift in the $^{31}P\{^1H\}$ NMR spectrum from 75.8 ppm to 77.0 ppm (Δδ = 1.2 ppm), but the change of the broad quartet signal of **1·BH₃** to a sharp singlet was indicative of loss of the quadrupolar boron centre. Removal of excess pyrrolidine *in vacuo* followed by filtration through a silica plug to remove pyrrolidine·$BH_3$ afforded **1** as a purple oil. The analogous deprotection of **2·BH₃** and **3·BH₃** afforded the free azophosphines **2** and **3**, respectively, and were accompanied by more significant changes in the $^{31}P\{^1H\}$ NMR chemical shifts on deprotection (Δδ = 9.8 ppm (**2**), and 8.6 ppm (**3**)). Interestingly, the *P*-aryl azophosphine **1** is significantly less stable in toluene solution than the *P*-alkyl analogue **2** (see Fig S1 and S2). Compound **2** is stable in the absence of air in toluene for several weeks with minimal decomposition, whereas **1** starts degrading within 24 hours (in both the light and the dark), and ultimately rearranges with loss of $N_2$ to afford $MesPPh_2$ as the major product as confirmed by NMR spectroscopy and mass spectrometry (Fig S1 and S3).

Single crystals of **3** suitable for single crystal X-ray diffraction were grown in the glovebox by slow

evaporation of *n*-hexane at −35 °C (Figure 2D). This pyramidal structure at phosphorus is reflected in the single crystal structure for **3**, in which the sum of the angles around P1 is 313.0°, with N1–N2 and N1–P1 bond lengths of 1.258(3) and 1.7494(18) Å, respectively. By contrast, the sum of the angles around the analogous nitrogen centre in related triazenes has been reported to be very close to 360°, with N=N bond lengths of 1.270(1) Å, 1.281(7) Å, and 1.288(6),[16] highlighting the increased planarisation in these species.

To probe the differences between azophosphine **3** and its N-containing analogue, triazene **A** (Table 1), density functional theory calculations and natural bond orbital (NBO) analyses were carried out (see SI for details). The computed bond metric data shows **3** has a shorter N=N bond (1.239 Å) than **A** (1.247 Å); this is corroborated by a Wiberg bond index (WBI) of 1.84 for the N=N bond of **3**, and 1.67 for **A**. Both metrics are consistent with reduced donation from the pnictogen lone pair into the N=N π* orbital for **3** compared to **A**. This was further supported by examination of the donor/acceptor interactions of the pnictogen lone pair into the N=N π* orbital; the value of 4.73 kcal·mol$^{-1}$ for **3** is significantly smaller than 79.58 kcal·mol$^{-1}$ for **A**. Additionally, the sum of the angles around the phosphorus centre in **3** (307.3°) is significantly lower than the angles around the nitrogen centre in **A** (357.6°), indicative of a pyramidal structure around the phosphorus centre, compared to the highly planarized triazene. This is consistent with the crystal structures discussed above.

**Table 1**. Key computational parameters for the comparison of **3** with N and C(H) analogues. WBI = Wiberg bond index.


E = P (**3**)
N (**A**)
C(H) (**B**)

| | **3** | **A** | **B** |
|---|---|---|---|
| WBI for N=N bond | 1.84 | 1.67 | 1.86 |
| N=N bond length (Å) | 1.239 | 1.247 | 1.232 |
| E lone pair to N=N π* donation (kcal·mol$^{-1}$) | 4.73 | 79.58 | - |
| Sum of angles around E (°) | 307.3 | 357.6 | - |

Given the aforementioned diagonal relationship between phosphorus and carbon,[2] **3** was also compared to carbon analogue **B** (Table 1). The computed N=N bond length (1.232 Å) and WBI (1.86) for **B** places **3** in between **A** and **B** for both. These values are consistent with **B** possessing significant N=N double bond character and N–C(H) single bond character (computed bond length of 1.465 Å). By contrast, the N=N bonds of **3** and **A** are both longer than the additive covalent radii for an N=N double bond, and the N–P/N–N bonds shorter, indicative of the increased delocalisation in these structures.[17] These data underlines the structure of **3** exists somewhere between that of triazene **A**, and the carbon equivalent **B**.

The availability of the phosphorus lone pair highlights the potential application of azophosphines as ligands. The P–N=N functionality classifies azophosphines as 1,3-P,N ligands. 1,3-P,N ligands display diverse coordination modes, including κ$^1$*N*, κ$^1$*P*, κ$^2$*P*,*N*, and μ*P*,*N*, and have applications in (cooperative) catalysis, bioinorganic chemistry and photoluminescence.[18] All previous examples of 1,3-P,N ligands feature C as the central element. However, control of the target coordination mode during synthesis, and subsequent isolation of the product, can be challenging.[19] We hypothesised the central nitrogen of azophosphines would reduce charge density at the terminal nitrogen and enable finer control of coordination mode.

The reaction of **2** with half an equivalent of the [Ru(*p*-cymene)Cl$_2$]$_2$ dimer (Scheme 3) was monitored by $^{31}$P{$^1$H} NMR spectroscopy, and clean conversion of the free azophosphine at 118.3 ppm to a new species at 121.7 ppm was observed. SXRD showed that this product was the half-sandwich piano stool complex Ru(*p*-cymene)(κ$^1$*P*-**2**)Cl$_2$ (**4**), which featured the azophosphine coordinated to the metal centre exclusively via the phosphine centre (Figure 3A). The only prior example of a coordinated azophosphine was the unexpected reaction of a PF$_3$ ligand in [RhCl(PF$_3$)(PPh$_3$)$_2$] with a silyldiazene, which generated the *P*,*P*-difluoroazophosphine PhN=NPF$_2$ bound to Rh; this product was only characterised by NMR spectroscopy and elemental analysis, but the results were consistent with P-coordination of the ligand.[20]

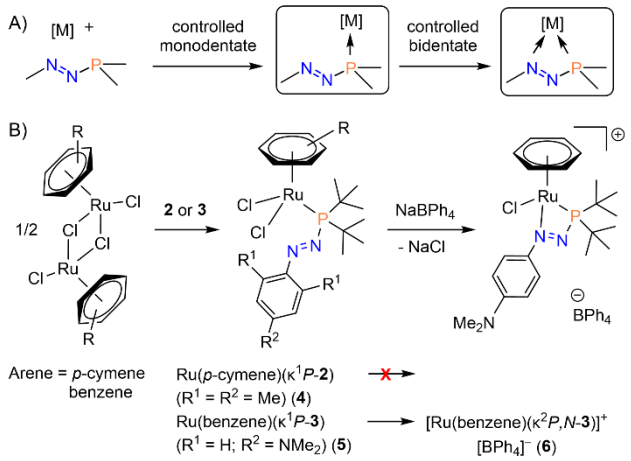


**Scheme 3.** Synthesis of Ru(arene) azophosphine complexes; Ru(p-cymene)(κ$^1$*P*-**2**) (**4**), Ru(benzene)(κ$^1$*P*-**3**) (**5**), [Ru(benzene)(κ$^2$*P*,*N*-**3**)][BPh$_4$] (**6**).

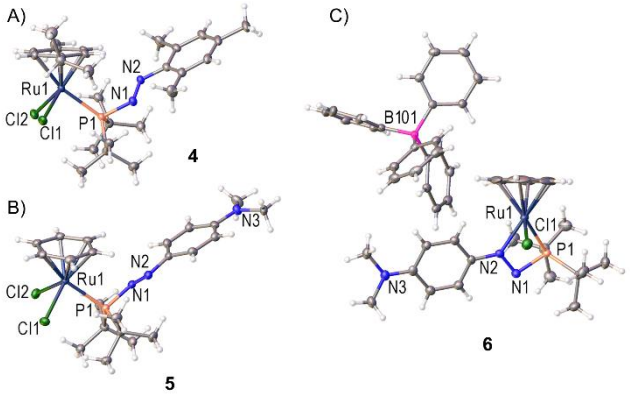


**Figure 2.** Single crystal structures of **4** (A); **5** (B); **6** (C). Selected bond distances (Å) and angles (°): **4** P1–Ru1 2.4208(7), P1–N1 1.777(2), N1–N1 1.258(3), P1–N1–N2 114.81(17); **5** P1–Ru1 2.4041(8), P1–N1 1.744(3), N1–N2 1.272(4), P1–N1–N2 118.3(2); **6** P1–Ru1 2.3607(6), P1–N1 1.749(2), N1–N2 1.300(3), P1–N1–N2 99.08(15), P1–Ru1–N2 62.62(6). Thermal ellipsoids were drawn at the 50% probability level.[14]

Attempts to generate a bidentate complex with ligand **2** via the terminal nitrogen by changing the temperature, solvent or using halide-extraction agents were unsuccessful. We reasoned this was not only due to the potentially weak binding of the nitrogen, but also the flanking steric bulk from the two *ortho*-methyl groups on the mesityl substituent, which would clash with the arene ring on the ruthenium on coordination. To circumvent this problem, we used azophosphine **3**, which has a smaller steric profile around the terminal nitrogen atom. The analogous reaction of **3** with the [Ru(benzene)Cl$_2$]$_2$ dimer revealed a similar small downfield shift in the $^{31}$P{$^1$H} NMR spectrum (107.7 ppm (**3**) to 111.9 ppm), indicative of κ$^1$*P* coordination of the ligand (Scheme 3). This was corroborated by single crystal X-ray diffraction, and showed that the compound has the composition Ru(benzene)(κ$^1$*P*-**3**)Cl$_2$ (**5**) (Figure 3B), which is structurally similar to **4**. Addition of NaBPh$_4$ to the chlorobenzene solution of **5** gave a brown precipitate, and extraction into dichloromethane left a white precipitate (NaCl). The $^{31}$P{$^1$H} NMR spectrum showed a significant upfield shift to 58.0 ppm. Single crystals suitable for analysis confirmed the bidentate nature of the ligand in the complex [Ru(benzene)(κ$^2$*P*,*N*-**3**)Cl][BPh$_4$] (**6**) (Figure 3C).

The P1–Ru1–N2 bite angle of 62.62(6)° in **6** is significantly shorter than those of prior Ru complexes of 1,3-P,N (range from 66.3(1)° to 69.80(6)°.[21] The P1–Ru1 bond length in **6** (2.3607(6) Å) is shortened relative to **5** (2.4041(8) Å), and the N1–N2 bond length is lengthened likely due to back-donation from Ru1 into the N-N π* orbital (1.300(3) Å and 1.272(4) Å, respectively). The ring strain in **6** is highlighted by the decreased P1–N1–N2 bond angle of 99.08(15)° from that of **5** (118.3(2)°). These single crystal structures demonstrate the κ$^1$*P* and κ$^2$*P*,*N* coordinative properties of azophosphines, in stark contrast to the triazene analogues. Variability of the P- and N-substituents provide scope for fine-tuning of electronics and sterics, thus encouraging further exploration of the coordination chemistry of azophosphines.

## Conclusions

In conclusion, we have developed a general synthetic route to azophosphines, *via* the corresponding azophosphine-borane, and probed the fundamental structure of these underexplored compounds. We have demonstrated controlled κ$^1$*P* and κ$^2$*P*,*N* coordination to Ru(II), highlighting a key difference between the P and N congeners. We are continuing to study the coordination chemistry and catalysis of azophosphines, and their potential to act as functionalised photoswitches.

## Acknowledgements

The authors would like to thank the Royal Society (URF\R1\201636), the EPSRC (EP/W036908/1), the

Wellcome Trust (204846/Z/16/Z), the University of Birmingham, and the NWO (Veni grant) for funding.

## References


[1] a) P. Floch, *Coord. Chem. Rev.* **2006**, *250*, 627-681; b) N. T. Coles, A. Sofie Abels, J. Leitl, R. Wolf, H. Grützmacher, C. Müller, *Coord. Chem. Rev.* **2021**, *433*; c) A. J. Ashe, *J. Am. Chem. Soc.* **2002**, *93*, 3293-3295; d) J. M. Goicoechea, H. Grützmacher, *Angew. Chem. Int. Ed.* **2018**, *57*, 16968-16994; e) A. R. Jupp, J. M. Goicoechea, *J. Am. Chem. Soc.* **2013**, *135*, 19131-19134; f) M. Regitz, *Chem. Rev.* **1990**, *90*, 191-213; g) J. G. Cordaro, D. Stein, H. Ruegger, H. Grutzmacher, *Angew. Chem. Int. Ed.* **2006**, *45*, 6159-6162; h) D. W. N. Wilson, S. J. Urwin, E. S. Yang, J. M. Goicoechea, *J. Am. Chem. Soc.* **2021**, *143*, 10367-10373.

[2] K. B. Dillon, F. Mathey, J. F. Nixon, *Phosphorus: The Carbon Copy: From Organophosphorus to Phospha-organic Chemistry*, John Wiley & Sons, **1998**.

[3] K. M. Szkop, A. R. Jupp, D. W. Stephan, *J. Am. Chem. Soc.* **2018**, *140*, 12751-12755.

[4] a) A. Khazaei, M. Kazem-Rostami, A. Zare, A. R. Moosavi-Zare, M. Sadeghpour, A. Afkhami, *J. Appl. Polym. Sci.* **2013**, *129*, 3439-3446; b) N. Lolak, S. Akocak, S. Bua, M. Koca, C. T. Supuran, *Bioorg. Chem.* **2018**, *77*, 542-547; c) S. Akocak, N. Lolak, S. Bua, C. T. Supuran, *J Enzyme Inhib Med Chem* **2018**, *33*, 1575-1580.

[5] a) A. A. Suleymanov, K. Severin, *Angew. Chem. Int. Ed.* **2021**, *60*, 6879-6889; b) D. B. Kimball, M. M. Haley, *Angew. Chem. Int. Ed.* **2002**, *41*, 3338-3351; c) R. Lazny, J. Poplawski, J. Köbberling, D. Enders, S. Bräse, *Synlett* **1999**, *1999*, 1304-1306.

[6] a) N. G. Connelly, G. Garcia, *J. Chem. Soc., Dalton Trans.* **1987**, 2737-2740; b) C. J. Adams, K. M. Anderson, R. A. Baber, N. G. Connelly, M. Kandiah, A. G. Orpen, *Dalton Trans* **2004**, 3353-3359; c) L. Carlton, M. S. Nyoni, M. A. Fernandes, *Polyhedron* **2016**, *119*, 194-201; d) C. Tejel, M. A. Ciriano, G. Rios-Moreno, I. T. Dobrinovitch, F. J. Lahoz, L. A. Oro, M. Parra-Hake, *Inorg. Chem.* **2004**, *43*, 4719-4726.

[7] a) G. Albertin, S. Antoniutti, M. Bedin, J. Castro, S. Garcia-Fontán, *Inorg. Chem.* **2006**, *45*, 3816-3825; b) A. G. Barrett, M. R. Crimmin, M. S. Hill, P. B. Hitchcock, G. Kociok-Kohn, P. A. Procopiou, *Inorg. Chem.* **2008**, *47*, 7366-7376; c) A. L. Johnson, A. M. Willcocks, S. P. Richards, *Inorg. Chem.* **2009**, *48*, 8613-8622.

[8] S. O. Hauber, F. Lissner, G. B. Deacon, M. Niemeyer, *Angew Chem Int Ed Engl* **2005**, *44*, 5871-5875.

[9] a) J. Kroner, W. Schneid, N. Wiberg, B. Wrackmeyer, G. Ziegleder, *J. Chem. Soc. Faraday Trans. 2* **1978**, *74*, 1909-1919; b) N. Wiberg, *Adv. Organomet. Chem.* **1984**, *23*, 131-191.

[10] O. A. Attanasi, P. Filippone, P. Guerra, F. Serra-zanetti, *Synth. Commun.* **1987**, *17*, 555-561.

[11] M. Y. Riu, W. J. Transue, J. M. Rall, C. C. Cummins, *J. Am. Chem. Soc.* **2021**, *143*, 7635-7640.

[12] K. Tanaka, M. Y. Riu, B. Valladares, C. C. Cummins, *Inorg. Chem.* **2022**, *61*, 13662-13666.

[13] a) A. E. Waked, R. Ostadsharif Memar, D. W. Stephan, *Angew. Chem. Int. Ed.* **2018**, *57*, 11934-11938; b) E. R. M. Habraken, N. P. van Leest, P. Hooijschuur, B. de Bruin, A. W. Ehlers, M. Lutz, J. C. Slootweg, *Angew. Chem. Int. Ed.* **2018**, *57*, 11929-11933; c) E. R. M. Habraken, L. J. C. van der Zee, K. N. A. van de Vrande, A. R. Jupp, M. Nieger, A. W. Ehlers, J. C. Slootweg, *Eur. J. Inorg. Chem.* **2019**, *2019*, 1594-1603.

[14] Deposition numbers 2190921 (for **1.BH3**), 2334072 (for **2.BH3**), 2334075 (for **3.BH3**), 2334076 (for **3**), 2334073 (for **4**), 2334074 (for **5**) and 2334077 (for **6**) contain the supplementary crystallographic data for this paper. These data are provided free of charge by the joint Cambridge Crystallographic Data Centre and Fachinformationszentrum Karlsruhe Access Structures service.

[15] G. C. Lloyd-Jones, N. P. Taylor, *Chem. Eur. J.* **2015**, *21*, 5423-5428.

[16] a) F. R. Fronczek, C. Hansch, S. F. Watkins, *Acta Crystallogr. C* **1988**, *44*, 1651-1653; b) C. Lego, B. Neumüller, *Z. Anorg. Allg. Chem.* **2011**, *637*, 1784-1789; c) S. L. Edwards, G. Chapuis, D. H. Templeton, A. Zalkin, *Acta Crystallogr. B* **1977**, *33*, 276-278.

[17] a) P. Pyykkö, M. Atsumi, *Chem. Eur. J.* **2008**, *15*, 186-197; b) P. Pyykkö, M. Atsumi, *Chem. Eur. J.* **2009**, *15*, 12770-12779; c) P. Pyykkö, *J. Phys. Chem. A* **2015**, *119*, 2326-2337.

[18] a) M. K. Rong, F. Holtrop, J. C. Slootweg, K. Lammertsma, *Coord. Chem. Rev.* **2019**, *380*, 1-16; b) M. K. Rong, F. Holtrop, J. C. Slootweg, K. Lammertsma, *Coord. Chem. Rev.* **2019**, *382*, 57-68.

[19] a) T. van Dijk, S. Burck, A. J. Rosenthal, M. Nieger, A. W. Ehlers, J. C. Slootweg, K. Lammertsma, *Chem. Eur. J.* **2015**, *21*, 9328-9331; b) M. K. Rong, K. van Duin, T. van Dijk, J. J. de Pater, B. J. Deelman, M. Nieger, A. W. Ehlers, J. C. Slootweg, K. Lammertsma, *Organometallics* **2017**, *36*, 1079-1090; c) M. K. Rong, F. Holtrop, E. O. Bobylev, M. Nieger, A. W. Ehlers, J. C. Slootweg, K. Lammertsma, *Chem. Eur. J.* **2021**, *27*, 14007-14016.

[20] J. F. Nixon, M. Kooti, *J. Organomet. Chem.* **1978**, *149*, 71-79.

[21] a) T. Oshiki, H. Yamashita, K. Sawada, M. Utsunomiya, K. Takahashi, K. Takai, *Organometallics* **2005**, *24*, 6287-6290; b) K. Wajda-Hermanowicz, Z. Ciunik, A. Kochel, *Inorg. Chem.* **2006**, *45*, 3369-3377; c) S. Pavlik, F. Jantscher, G. Dazinger, K. Mereiter, K. Kirchner, *Eur. J. Inorg. Chem.* **2006**, *2006*, 1006-1021; d) P. Kumar, A. K. Singh, M. Yadav, P.-z. Li, S. K. Singh, Q. Xu, D. S. Pandey, *Inorg. Chim. Acta* **2011**, *368*, 124-131; e) R. García-Álvarez, S. E. García-Garrido, J. Díez, P. Crochet, V. Cadierno, *Eur. J. Inorg. Chem.* **2012**, *2012*, 4218-4230; f) E. Essoun, R. Wang, M. A. S. Aquino, *Inorg. Chim. Acta* **2017**, *454*, 97-106.